EFFECTS OF APPROXIMATIONS ON THE STATIC AND DYNAMIC RESPONSE OF A CANTILEVER WITH A TIP MASS

MARCELO R. M. CRESPO DA SILVA and CLIFFORD L. ZARETZKY
Department of Mechanical Engineering. Aeronautical Engineering and Mechanics,
Rensselaer Polytechnic Institute. Troy. NY 12180-3590. U.S.A.

and

DEWEY H. HODGES
School of Aerospace Engineering. Georgia Institute of Technology. Atlanta. GA 30332-0150.
U.S.A.

Abstract—The problem of determining the equilibrium deflections of a beam with a tip mass, and the frequency of infinitesimally small oscillations about the beam's equilibrium state, E, is analyzed. The beam is able to experience flexure along two normal directions in space (thus, flexure in any direction) and torsion. Numerical solutions of the full, nonlinear beam static equilibrium equations are obtained by direct integration of a two-point boundary value problem. The results obtained are compared with an approximate perturbation expansion solution, E^*, for the equilibrium state E. The frequencies associated with the small oscillations about the equilibrium state are determind by linearizing the equations of motion about the equilibrium state, and by using a transfer matrix technique on the resulting equations. The effect on the calculated frequencies of using the approximate solution E^*, obtained by a perturbation method (instead of the more exact numerical solution E mentioned above) in the linearized equations, is assessed. The use of an alternative way to determine an approximation for the natural frequencies of the system is also assessed. For this, small motions are assumed and the equations of motion are first expanded about the undeformed state of the beam. The undeformed state is not a static equilibrium state if gravity is considered. The resulting equations, which contain only polynomial nonlinearities, are then used to analyze the motion. After the equilibrium solution to these equations, E^* is determined by a perturbation expansion; these same equations are then linearized about E^* and the natural frequencies are also determined by a transfer matrix technique. It is shown that the approximation so obtained for the natural frequencies can be unsatisfactory for large values of the tip mass. All the results obtained in this paper are compared with published finite elements and with experimental results.

INTRODUCTION

Generally, a structure such as a beam can respond to external loads by exhibiting flexure in any direction in space and torsion. For infinitesimally small deformations of prismatic beams, the linear equations of motion disclose that flexural motions along the two principal directions are uncoupled. Moreover, if the axis of cross-sectional mass centers coincides with the elastic axis, the linearized flexural and torsional motions are also uncoupled.

The investigation of the response of dynamical systems involves the determination of eigenvalues associated with infinitesimally small motions about the system's equilibrium states. When an equilibrium state is "small", one could determine such frequencies by first replacing the full nonlinear differential equations of motion by a set of equations with polynomial nonlinearities, truncated to a certain degree, and then applying Galerkin's method to the resulting equations. With N appropriate functions being chosen for the Galerkin procedure, both the equilibrium solution and the eigenvalues associated with the perturbed motion would be determined for increasing values of N until convergence is achieved (see, for example, Ormiston and Hodges. 1972; Dowell *et al.*, 1977; Crespo da Silva and Hodges, 1986). It should be noted that the results so obtained also depend on the order of truncation of the expanded equations. For larger equilibrium solutions, one would expect that higher and higher order terms would have to be retained in the expanded equations, in order to increase the accuracy of the results. Thus, to be strict, one should also experiment with the level of truncation of the expanded equations in order to verify convergence of the results.
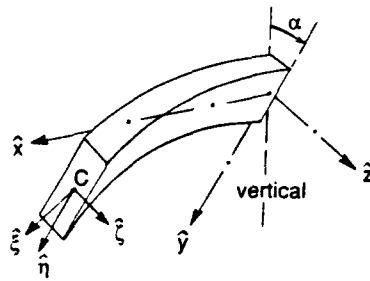
Fig. 1. A beam segment, the inertial unit vector triad ($\hat{x}, \hat{y}, \hat{z}$), and the section-fixed unit vector triad ($\hat{\xi}, \hat{\eta}, \hat{\zeta}$).

In the present work, the problem of determining the natural frequencies associated with infinitesimally small flexural–flexural oscillations of a beam with a tip mass is addressed. Special attention is given to the process of expanding the governing differential equations of motion of the beam to determine the natural frequencies. This paper is organized in the following way. First, the nonlinear equations of motion that are valid for arbitrary motion (except that the strain must be small) involving bending/bending are formulated. Next, the equilibrium configuration is determined from two methods: (1) from a numerical solution of the two-point boundary value problem associated with the static part of the full nonlinear equations of motion; and (2) from an approximate perturbation expansion of the static part of the equations of motion about the undeformed state of the beam. The results obtained are compared with each other, with experimental data available in Dowell and Traybar (1975a,b) and Dowell et al. (1977), and with a finite element analysis presented in Hinnant and Hodges (1987) and Bauchau and Liu (1989). The natural frequencies associated with infinitesimally small oscillations about the equilibrium state of the beam are determined by a transfer matrix method, based on a set of coupled equations obtained by expansion of the full nonlinear differential equations of motion about their equilibrium solution. This is done in the section entitled "Response Analysis". Following this, the accuracy of analyzing the motion with a set of nonlinear approximate equations, expanded about the undeformed state of the beam, is then assessed.

EQUATIONS OF MOTION

The differential equations governing the flexural-flexural-torsional motion of inextensional beams, taking into account all the geometric nonlinearities in the system, were formulated in Crespo da Silva and Glynn (1978a,b), and in Crespo da Silva (1988a,b) for both extensional and inextensional beams. For the sake of completeness, a brief derivation of the equations for an inextensional beam with a tip mass is presented below.

The beam is assumed to be initially straight and untwisted, of length l, and of constant mass m per unit length and constant stiffness $D_\eta = EI_\eta$, $D_\zeta = EI_\zeta$ and $D_\xi = GJ$. The quantities D_η and D_ζ, where E is Young's modulus for the material, and I_η and I_ζ are principal cross-sectional area moments of inertia, are the bending stiffnesses for the beam while GJ is its torsional stiffness. A schematic of the deformed beam is shown in Fig. 1. Let $hu(s, t)$, $hv(s, t)$ and $hw(s, t)$ denote the components along the inertial directions (x, y, z) of the displacement of the beam's centroidal axis C (which is assumed to be coincident with the beam's elastic axis) of a cross-section S due to elastic deformation of the beam. Here, the unit vectors along any direction are denoted with "hats" ($\hat{x}$ along x, etc.) as shown in Fig. 1; s is used to denote arc-length along the beam, non-dimensionalized by l; and t is the normalized time given by $t = \tau\sqrt{D_\eta/(ml^4)}$ where τ is used to denote dimensional time. For inextensional beams, $(1+u')^2+v'^2+w'^2 = 1$ where $( )' = \partial( )/\partial s$. A lumped mass M, of weight Mg, is located at the beam's tip at $s = 1$. As can be inferred from Fig. 1, the gravitational force applied at $s = 1$ is equal to $Mg[\hat{v}\cos\alpha+\hat{z}\sin\alpha]$, where α is the angle from the vertical axis to the direction $\hat{v} = \hat{\eta}(0, t)$. Therefore, the virtual work associated with the tip mass is equal to $Mg[(\cos\alpha)\,\delta v(1, t)+(\sin\alpha)\,\delta w(1, t)]$.
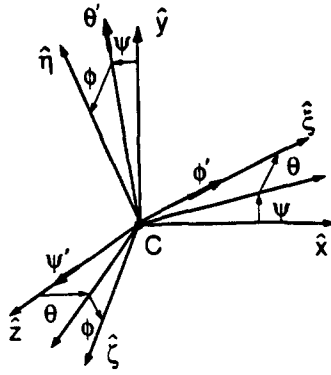
Fig. 2. Angles (ψ, θ, ϕ) used to describe the orientation of $(\hat{\xi}, \hat{\eta}, \hat{\zeta})$ relative to $(\hat{x}, \hat{y}, \hat{z})$.

The unit vectors $[\hat{\xi}(s, t), \hat{\eta}(s, t), \hat{\zeta}(s, t)]$ are aligned with the principal axes of the beam's cross-section S at an arbitrary station s, when the beam is undeformed (and if warping were neglected). The orientation of the unit vector triad $(\hat{\xi}, \hat{\eta}, \hat{\zeta})$ relative to the inertial unit vector triad $(\hat{x}, \hat{y}, \hat{z})$ is described by the three successive rotations $[\psi(s, t), \theta(s, t), \phi(s, t)]$ shown in Fig. 2. If the effect of shear is neglected, it follows that

$$\tan \psi = \frac{v'}{1 + u'}$$

$$\tan \theta = -\frac{w'}{\sqrt{(1 + u')^2 + v'^2}}. \tag{1}$$

Letting $\beta_v = D_\zeta/D_\eta$ and $\beta_\gamma = D_\zeta/D_\eta$, the differential equations of motion can be obtained from Hamilton's extended principle as in Crespo da Silva and Glynn (1978a), i.e.

$$\delta I = \delta \int_{t_1}^{t_2} \int_0^1 \left\{ L(\psi, \theta, \phi, \psi', \theta', \phi', \ddot{u}, \ddot{v}, \ddot{w}) + \frac{\lambda}{2} [1 - (1 + u')^2 - v'^2 - w'^2] \right\} ds \, dt$$

$$+ \int_{t_1}^{t_2} \left\{ \frac{M}{ml} [\ddot{u}\delta u + \ddot{v}\delta v + \ddot{w}\delta w] + P(\delta v \cos \alpha + \delta w \sin \alpha) \right\}_{s=1} dt = 0, \tag{2}$$

where λ is a Lagrange multiplier,

$$P = Mgl^2/D_\eta \quad \text{and} \quad L = \tfrac{1}{2}(\ddot{u}^2 + \ddot{v}^2 + \ddot{w}^2) + \frac{ml}{M} P(v \cos \alpha + w \sin \alpha) - \tfrac{1}{2}(\rho_\eta^2 + \beta_\gamma \rho_\zeta^2 + \beta_\gamma \rho_\zeta^2)$$

is the specific Lagrangean for the motion, normalized by D_η/l^2. Dots denote differentiation with respect to non-dimensional time t. In the expression for the Lagrangean, ρ_η and ρ_ζ are bending curvature components associated with the $\hat{\eta}$ and $\hat{\zeta}$ directions, respectively, and ρ_ξ is the torsion, each normalized by $1/l$. The expression for the normalized curvature vector, $\rho = \rho_\xi \hat{\xi} + \rho_\eta \hat{\eta} + \rho_\zeta \hat{\zeta}$, obtained by inspection of Fig. 2, is given by

$$\rho = (\phi' - \psi' \sin \theta)\hat{\xi} + (\psi' \cos \theta \sin \phi + \theta' \cos \phi)\hat{\eta} + (\psi' \cos \theta \cos \phi - \theta' \sin \phi)\hat{\zeta}. \tag{3}$$

For simplicity, it is assumed that the beam is slender and that its torsional frequencies are much higher than its flexural frequencies, so that the small effects of rotary inertia and torsional dynamics are neglected in eqn (2). The mass moments and products of inertia of the tip mass are also neglected for simplicity. By carrying out the variations in eqn (2), the differential equations of motion and a boundary condition equation governing the motion of the beam are readily obtained. The normalized differential equations of motion are

$$G'_u \triangleq \left[A_\psi \frac{\partial \psi}{\partial u'} + A_\theta \frac{\partial \theta}{\partial u'} + \lambda(1+u') \right]' = \ddot{u}$$

$$G'_v \triangleq \left(A_\psi \frac{\partial \psi}{\partial v'} + A_\theta \frac{\partial \theta}{\partial v'} + \lambda v' \right)' = \ddot{v} - \frac{ml}{M} P \cos \alpha$$

$$G'_w \triangleq \left(A_\psi \frac{\partial \psi}{\partial w'} + A_\theta \frac{\partial \theta}{\partial w'} + \lambda w' \right)' = \ddot{w} - \frac{ml}{M} P \sin \alpha, \tag{4}$$

and

$$A_\phi = 0. \tag{5}$$

The boundary condition equation obtained from eqn (2) can be written as

$$\left\{ \beta_z(\phi' - \psi' \sin \theta) \delta\phi + \left(G_u + i \frac{M}{ml} \ddot{u} \right) \delta u + \left(G_v + i \frac{M}{ml} \ddot{v} - iP \cos \alpha \right) \delta v \right.$$

$$+ \left(G_w + i \frac{M}{ml} \ddot{w} - iP \sin \alpha \right) \delta w - \left(H_v - \frac{v'H_u}{1+u'} \right) \delta v'$$

$$\left. - \left(H_w - \frac{w'H_u}{1+u'} \right) \delta w' \right\}_{s=i} = 0, \quad i = 0, 1. \tag{6}$$

In the above equations

$$A_k = \left(\frac{\partial L}{\partial k'} \right)' - \frac{\partial L}{\partial k} \quad \text{(for } k = \psi, \theta, \phi) \tag{7}$$

and

$$H_k = \frac{\partial L}{\partial \psi'} \frac{\partial \psi}{\partial k'} + \frac{\partial L}{\partial \theta'} \frac{\partial \theta}{\partial k'} \quad \text{(for } k = u, v, w). \tag{8}$$

The functions A_ψ, A_θ and A_ϕ are given as

$$A_\psi = [\beta_z \rho_z \sin \theta - \rho_\eta \cos \theta \sin \phi - \beta_y \rho_z \cos \theta \cos \phi]'$$

$$A_\theta = (\beta_z \rho_z \sin \phi - \rho_\eta \cos \phi)' - \psi'[\beta_z \rho_z \cos \theta + \rho_\eta \sin \theta \sin \phi + \beta_y \rho_z \sin \theta \cos \phi]$$

$$A_\phi = -\beta_z \rho'_z - (\beta_y - 1)\rho_\eta \rho_z. \tag{9}$$

Equations (4), (5) and (6), and the constraint relation, $(1+u')^2 + v'^2 + w'^2 = 1$, govern the flexural-flexural motions of a beam with a tip mass when the torsional frequencies are much higher than the bending frequencies.

By making use of the cantilever boundary condition $G_u(1, t) = -(M/ml)\ddot{u}(1, t)$, the first of eqns (4) can be integrated once to yield

$$\lambda(s, t) = -\frac{1}{1+u'} \left[\int_s^1 \ddot{u}(x, t) \, dx + \frac{M}{ml} \ddot{u}(1, t) + A_\psi \frac{\partial \psi}{\partial u'} + A_\theta \frac{\partial \theta}{\partial u'} \right]. \tag{10}$$

With ψ and θ given by eqns (1), substitution of eqn (10) into the second and third of eqns (4) yields the following integro-partial differential equations for $v(s, t)$ and $w(s, t)$:

$$\left\{\frac{1}{1+u'}\left[A_\psi - v'\left(\int_s^1 \ddot{u}(y,t)\,dy + \frac{M}{ml}\ddot{u}(1,t)\right)\right]\right\}' \triangleq G_v'(s,t) = \ddot{v} - \frac{ml}{M}P\cos\alpha$$

$$\left\{\frac{v'w'A_\psi}{(1+u')(1-w'^2)} - \frac{A_\theta}{\sqrt{1-w'^2}} - \frac{w'}{1+u'}\left(\int_s^1 \ddot{u}(y,t)\,dy + \frac{M}{ml}\ddot{u}(1,t)\right)\right\}'$$

$$\triangleq G_w'(s,t) = \ddot{w} - \frac{ml}{M}P\sin\alpha. \quad (11)$$

The boundary conditions for eqns (11) and (5), obtained directly from eqn (6), are

$$v(0,t) = w(0,t) = v'(0,t) = w'(0,t) = \phi(0,t) = \rho_\eta(1,t) = \rho_\zeta(1,t) = \rho_\xi(1,t) = 0,$$

$$G_w(1,t) = p_w - \frac{M}{ml}\ddot{w}(1,t) \quad \text{and} \quad G_v(1,t) = \beta_y p_v - \frac{M}{ml}\ddot{v}(1,t).$$

where p_w and p_v are defined as $p_w = P\sin\alpha$ and $p_v = (P/\beta_y)\cos\alpha$.
With $u(0,t) = 0$, the inextensibility condition yields for $u(s,t)$,

$$u(s,t) = \int_0^s \left(\sqrt{1-v'^2-w'^2}-1\right)ds. \quad (12)$$

For the perturbation solution developed later, the variable $\phi(s,t)$ can be eliminated from eqns (11) by integrating eqn (5) with the boundary conditions $\rho_\zeta(1,t) = 0$ and $\phi(0,t) = 0$ to obtain,

$$\rho_\zeta = \phi' - \psi'\sin\theta = -\frac{\beta_y-1}{\beta_y}\int_s^1 \rho_\eta(x,t)\rho_\zeta(x,t)\,dx \quad (13)$$

so that

$$\phi(s,t) = \int_0^s \psi'(x,t)\sin\theta(x,t)\,dx - \frac{\beta_y-1}{\beta_y}\int_0^s\int_y^1 \rho_\eta(x,t)\rho_\zeta(x,t)\,dx\,dy. \quad (14)$$

In the next sections, the equilibrium state of the beam and the natural frequencies associated with infinitesimally small motions about the equilibrium are determined.

RESPONSE ANALYSIS

To analyze the motion governed by eqns (11) and (5), the normalized deformations $v(s,t)$ and $w(s,t)$, and the angle $\phi(s,t)$ are expressed as

$$v(s,t) = v_e(s) + v_s(s,t)$$
$$w(s,t) = w_e(s) + w_s(s,t)$$
$$\phi(s,t) = \phi_e(s) + \phi_s(s,t), \quad (15)$$

where $v_s(s,t)$, $w_s(s,t)$, and $\phi_s(s,t)$, denote infinitesimally small perturbations about the equilibrium solution (v_e, w_e, ϕ_e). The subscript "e" will be used from now on to denote an equilibrium value for the corresponding time dependent variable

Equilibrium solution E
    The equilibrium solution, E, satisfies the differential equations of motion with the dynamic terms in eqns (11) identically equal to zero. With the boundary conditions $G_{ve}(1) = \beta_y p_v$ and $G_{we}(1) = p_w$, eqns (11) can be integrated once to yield

$$\frac{A_{\psi e}}{1+u'_e} \triangleq G_{ve}(s) = \beta_y p_v \left[1 + \frac{ml}{M}(1-s)\right]$$

$$\frac{\beta_y p_v \left[1 + \dfrac{ml}{M}(1-s)\right] v'_e w'_e}{1 - w'^2_e} - \frac{A_{\theta e}}{\sqrt{1 - w'^2_e}} \triangleq G_{we}(s) = p_w \left[1 + \frac{ml}{M}(1-s)\right]. \qquad (16)$$

Equations (16) and (5) are a set of nonlinear, ordinary differential equations that will be solved with the boundary conditions $v_e(0) = w_e(0) = v'_e(0) = w'_e(0) = \phi_e(0) = 0$, and $\psi'_e(1) = \theta'_e(1) = \phi'_e(1) = 0$. To determine the equilibrium solution for the beam, a numerical solution to these equations is sought. For this, it is convenient to express these equations in terms of the angles $[\psi_e(s), \theta_e(s), \phi_e(s)]$. Since

$$v'_e = \cos \theta_e \sin \psi_e$$

$$w'_e = -\sin \theta_e. \qquad (17)$$

eqns (16) and (5) may be written as

$$(\beta_z \rho_{\zeta e} \sin \theta_e - \rho_{\eta e} \cos \theta_e \sin \phi_e - \beta_y \rho_{\zeta e} \cos \theta_e \cos \phi_e)' - \beta_y p_v \left[1 + \frac{ml}{M}(1-s)\right] \cos \psi_e \cos \theta_e = 0$$

$$(\rho_{\eta e} \cos \phi_e - \beta_z \rho_{\zeta e} \sin \phi_e)' + (\beta_z \rho_{\zeta e} \cos \theta_e + \rho_{\eta e} \sin \theta_e \sin \phi_e$$

$$+ \beta_y \rho_{\zeta e} \sin \theta_e \cos \phi_e)\psi'_e - (\beta_y p_v \sin \theta_e \sin \psi_e + p_w \cos \theta_e)\left[1 + \frac{ml}{M}(1-s)\right] = 0$$

$$\beta_z \rho'_{\zeta e} + (\beta_y - 1)\rho_{\eta e} \rho_{\zeta e} = 0, \qquad (18)$$

where $\rho_{\zeta e}, \rho_{\eta e}, \rho_{\zeta e}$ are the normalized curvature components at equilibrium obtained directly from eqn (3).

The determination of the equilibrium state of the system is now reduced to a two-point boundary-value problem requiring the integration of eqns (18), in conjunction with eqns (17) to determine the static equilibrium deflections $v_e(s)$ and $w_e(s)$. To this end, the following states are introduced

$$x_1 = v_e; \quad x_2 = w_e$$

$$x_3 = \psi_e; \quad x_4 = \theta_e; \quad x_5 = \phi_e; \quad x_6 = \gamma_e$$

$$x_7 = \psi'_e; \quad x_8 = \theta'_e; \quad x_9 = \phi'_e \qquad (19)$$

with the boundary conditions $x_i(0) = 0$ for $i = 1, \ldots, 6$ and $x_7(1) = x_8(1) = x_9(1) = 0$. The state equations $x'_i = f_i(x_1, \ldots, x_9)$ were integrated numerically using the double precision IMSL routine DBVPFD (IMSL, 1987). The state $x_6 = \gamma_e$, with $x'_6 = \rho_{\zeta e}(s)$, was introduced as a convenient way to determine the elastic angle of twist $\gamma_e(s)$. The routine DBVPFD divides the interval $0 \leqslant s \leqslant 1$ in a number of grid points, N, and computes the solution until its estimated error is smaller than a specified value. The results obtained were essentially insensitive to values of the error parameter smaller than about 10^{-4} and for N greater than about 20. Values of 10^{-8} and 40, respectively, were used for these parameters. These values provided at least six digit accuracy in the integration of the above differential equations.

In order to assess the influence of approximations on the equilibrium solution and on the calculation of the natural frequencies of the system, an approximate solution, E^*, to eqns (16) and eqns (5) is also generated by a perturbation technique. For this, the equilibrium deflections are assumed to be small and are expanded in a "book-keeping parameter" ε as

$v_e(s) = \varepsilon v_{e1}(s) + \varepsilon^2 v_{e2}(s) + \cdots$, $w_e(s) = \varepsilon w_{e1}(s) + \varepsilon^2 w_{e2}(s) + \cdots$. Since eqn (14) discloses that $\phi = O(\varepsilon^2)$, one then lets $\phi_e(s) = \varepsilon^2 \phi_{e2} + \cdots$. With $p_c = \varepsilon p_{r1}$ and $p_w = \varepsilon p_{w1}$, eqns (16) then yield a set of differential equations for the variables v_{e1}, w_{e1}, etc. which are obtained by equating the coefficients of equal powers of ε to zero in the expanded equations. By applying the given boundary conditions at the $O(\varepsilon)$ level, the solutions for $v_{e1}(s)$ and $w_{e1}(s)$ are

$$v_{e1}(s) = p_{r1}\left[s^2/2 - s^3/6 + \frac{ml}{M}\frac{s^2}{24}(s^2 - 4s + 6) \right]$$

and

$$w_{e1}(s) = p_{w1}\left[s^2/2 - s^3/6 + \frac{ml}{M}\frac{s^2}{24}(s^2 - 4s + 6) \right].$$

The solutions for the differential equations at the $O(\varepsilon^j)$ level depend on the solution obtained from the previous levels. Dropping the book-keeping parameter ε for convenience, the $O(\varepsilon^3)$ solutions for $v_e(s)$ and $w_e(s)$, which were obtained with the aid of MACSYMA (Pavelle and Wang, 1985; Symbolics, 1987; Rand, 1984), are

$$v_e(s) = \tfrac{1}{2}p_r s^2 \left[1 - \frac{s}{3} + \frac{ml}{12M}(s^2 - 4s + 6) \right] + \frac{p_r^3 s^2}{840}(3s^5 - 21s^4 + 49s^3 - 35s^2 - 28)$$

$$- \frac{p_r p_w^2 s^2}{5040\beta_y}\left[(5 - 23\beta_y)s^5 + (161\beta_y - 35)s^4 + (126 - 420\beta_y)s^3 \right.$$

$$+ (490\beta_y - 280)s^2 + 280(1 - \beta_y)s + 158\beta_y$$

$$\left. - \frac{10(\beta_y - 1)^2}{\beta_y}(s^5 - 7s^4 + 21s^3 - 35s^2 + 28s) \right] + O(\varepsilon^3) \text{ terms in } \frac{ml}{M},$$

$$w_e(s) = \tfrac{1}{2}p_w s^2 \left[1 - \frac{s}{3} + \frac{ml}{12M}(s^2 - 4s + 6) \right] + \frac{p_w^3 s^2}{840}(3s^5 - 21s^4 + 49s^3 - 35s^2 - 28)$$

$$- \frac{p_w p_r^2 s^2}{5040}\left[(5\beta_y - 23)s^5 + (161 - 35\beta_y)s^4 + (126\beta_y - 420)s^3 \right.$$

$$+ (490 - 280\beta_y)s^2 + 280(\beta_y - 1)s + 168$$

$$\left. - \frac{10(\beta_y - 1)^2}{\beta_y}(s^5 - 7s^4 + 21s^3 - 35s^2 + 28s) \right] + O(\varepsilon^3) \text{ terms in } \frac{ml}{M}. \tag{20}$$

From eqns (14) and (3), the corresponding $O(\varepsilon^3)$ solution for the beam's torsion described in terms of its elastic angle of twist γ_e is

$$\gamma_e(s) \triangleq \int_0^s \rho_e(\eta)\,d\eta = \frac{p_r p_w (\beta_y - 1)}{\beta_y}\left\{ \frac{(s-1)^4 - 1}{12} - \frac{ml}{M}\frac{(s-1)^5 + 1}{20} + \left(\frac{ml}{M}\right)^2\frac{(s-1)^6 - 1}{120} \right\}. \tag{21}$$

To $O(\varepsilon^3)$, the angle ϕ_e is given by

$$\phi_e(s) = \gamma_e(s) - \int_0^s v_e''(\eta)w_e'(\eta)\,d\eta = \gamma_e(s) - \frac{p_r p_w s^2}{8}\left[s - 2 - 4\left(\frac{ml}{M}\right)(s^2 - 3s + 3) \right]^2. \tag{22}$$

The $O(\varepsilon^3)$ terms in ml/M in eqns (20) are quite lengthy and, for this reason, are not reproduced here. If the terms in ml/M are neglected, the above $O(\varepsilon^3)$ solutions are the same
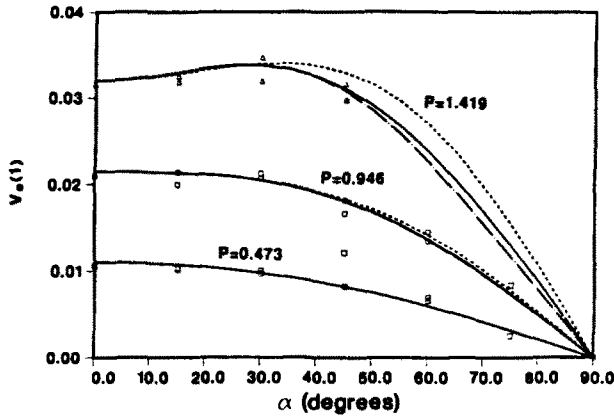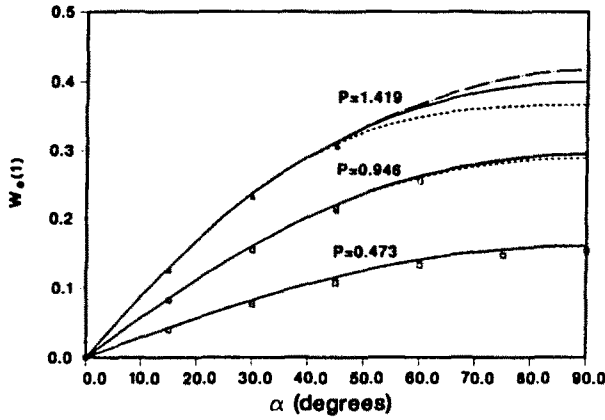
Fig. 3. Equilibrium tip deflection $v_e(1)$ versus the angle α for $D_\eta/(mgl^3) = 16.69$ and $P = 0.473$, 0.946 and 1.419 [——— eqns (17) and (18) ; --- $O(\varepsilon^3)$; —·—·— $O(\varepsilon^5)$].

Fig. 4. Equilibrium tip deflection $w_e(1)$ versus the angle α for $D_\eta/(mgl^3) = 16.69$ and $P = 0.473$, 0.946 and 1.419 [——— eqns (17) and (18) ; --- $O(\varepsilon^3)$; —·—·— $O(\varepsilon^5)$].
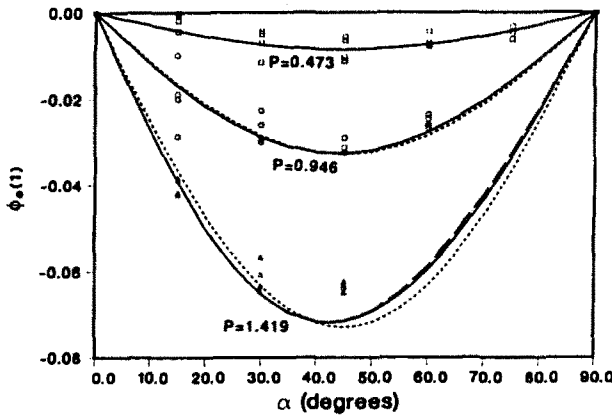
Fig. 5. Angle $\phi_e(1)$, versus the angle α for $D_\eta/(mgl^3) = 16.69$ and $P = 0.473$, 0.946 and 1.419 [——— eqns (17) and (18) ; --- $O(\varepsilon^3)$; —·—·— $O(\varepsilon^5)$].

ones obtained in Hodges *et al.* (1988). For large tip masses, the effect of these terms is very small. To assess the accuracy of the perturbation solution, an $O(\varepsilon^5)$ equilibrium solution for tip weights up to about 24 times the weight of the beam, was also generated with the aid of MACSYMA.

Figures 3–5 display the equilibrium tip deflections $v_e(1)$, $w_e(1)$ and $\phi_e(1)$ versus α for

$$\beta_x = 15.02, \quad \beta_z = 1.247, \quad \frac{M}{ml} = \frac{D_t}{mgl^3}, \quad P = 16.69P$$

and for the values of P indicated. The parameter values indicated match the values in Hinnant and Hodges (1987), for an aluminum beam of rectangular cross-section, with a heavy tip mass, used in the experiments reported in Dowell and Traybar (1975a,b), and in Dowell *et al.* (1977). The experimental points are included in these figures. The values of $P = 0.473$, 0.946 and 1.419 correspond, respectively, to tip weights of 1, 2 and 3 lb, used in the experiments, which are about eight, 16, and 24 times the weight of the beam. In Fig. 5, the third orientation angle $\phi_c(1)$ [instead of the actual torsion $\gamma_c(1)$] is plotted since it corresponds to the $O(\varepsilon^3)$ approximation for the angle measured in Dowell *et al.* (1977) [see the first of eqn (23) in Hodges *et al.* (1988)].

The numerical solutions of eqns (16) and (5) shown in Figs 3–5 agree with the results of a finite element analysis presented in Hinnant and Hodges (1987). They also agree with the results of a finite element analysis presented in Bauchau and Liu (1989). The perturbation and the numerical results are also in very close agreement with the experimental results mentioned above. In addition, the results obtained by neglecting the terms in ml/M are nearly indistinguishable from those shown in the figures. For smaller values of P, the simpler, $O(\varepsilon^3)$ solution is in very good agreement with the numerical solution. As seen in Fig. 4, the beam's tip deflection when $\alpha = 90^\circ$ and $P = 1.419$ is about 40% of the length of the beam. Even for such a large deflection, the error of the $O(\varepsilon^3)$ approximate solution is only about 8%.

Natural frequencies

To determine the natural frequencies ω_i associated with infinitesimally small motions about the equilibrium state of the beam, eqns (11) and (5) are linearized about the equilibrium determined above. For this, let

$$\psi(s,t) = \psi_c(s) + \psi_s(s,t)$$

$$\theta(s,t) = \theta_c(s) + \theta_s(s,t)$$

$$\phi(s,t) = \phi_c(s) + \phi_s(s,t). \tag{23}$$

With $G_t(s,t) \triangleq G_{tc}(s) + G_{ts}(s,t)$, $G_w(s,t) \triangleq G_{wc}(s) + G_{ws}(s,t)$ and $A_\phi(s,t) \triangleq A_{\phi c}(s) + A_{\phi s}(s,t)$, the following expressions for G_{ts}, G_{ws} and A_ϕ are obtained by linearizing eqns (11) and (5) in the infinitesimally small perturbations $\psi_s(s,t)$, $\theta_s(s,t)$ and $\phi_s(s,t)$:

$$G_{ts} = \frac{1}{\cos\theta_c \cos\psi_c}(t_1\theta_s + t_2\phi_s + t_3\theta'_s + t_4\psi'_s + t_5\phi'_s)' + \frac{\beta_y p_c\left[1 + \frac{ml}{M}(1-s)\right]}{\cos\theta_c \cos\psi_c} g(s,t)$$

$$+ \tan\psi_c\left[\int_s^1 \int_0^v \ddot{g}(x,t)\,dx\,dy + \frac{M}{ml}\int_0^1 \ddot{g}(s,t)\,ds\right],$$

$$G_{ws} = -\beta_y p_c\left[1 + \frac{ml}{M}(1-s)\right]\left(\theta_s\frac{\sin\psi_c}{\cos^2\theta_c} + \psi_s\cos\psi_c\tan\theta_c\right) - (\sin\psi_c\tan\theta_c)G_{tc}$$

$$- \frac{1}{\cos\theta_c}[(t_6\theta_s + t_7\phi_s + t_8\theta'_s + t_9\psi'_s)' + t_9\theta_s + t_{10}\phi_s - t_6\theta'_s - t_{11}\psi'_s + t_{11}\phi'_s]$$

$$- \cos\psi_c\tan\theta_c\left[\int_s^1 \int_0^v \ddot{g}(x,t)\,dx\,dy + \frac{M}{ml}\int_0^1 \ddot{g}(s,t)\,ds\right]$$

$$A_{\phi c} = t_{12}\theta_s + t_{13}\phi_s + t_{14}\theta'_s + t_{15}\psi'_s - t_5\psi''_s + \beta_z\phi''_s = 0. \tag{24}$$

where

$$g(s, t) = \psi_s \sin \psi_e \cos \theta_e + \theta_s \cos \psi_e \sin \theta_e. \tag{25}$$

The coefficients t_i, for $i = 1, \ldots, 15$, are functions of the equilibrium values of the deformation variables only. Their expressions are given in the Appendix.

To calculate the frequencies ω_i, one could make use of a number, N, of cantilever modes for $M = 0$, as in Hodges and Ormiston (1976), to replace the linearized counterpart of eqns (11) and (5) by $3N$ second-order differential equations. In this paper, the frequencies ω_i are determined by direct numerical integration of a two-point boundary value problem and by using a transfer matrix technique, as outlined below. The advantage of doing so is that one can circumvent a series representation for the field variables and directly obtain a set of eigenfunctions. Each eigenfunction determined in this manner represents the linearized motion for a particular mode.

By assuming a solution to the linearized equations as

$$\psi_s(s, t) = F_\psi(s)\, e^{i\omega t}$$

$$\theta_s(s, t) = F_\theta(s)\, e^{i\omega t}$$

$$\phi_s(s, t) = F_\phi(s)\, e^{i\omega t}, \tag{26}$$

and by writing $G_{rs}(s, t) = F_{G_{rs}}(s)\, e^{i\omega t}$, and $G_{ws}(s, t) = F_{G_{ws}}(s)\, e^{i\omega t}$, the following ordinary differential equations for the functions $F_\psi(s)$, $F_\theta(s)$ and $F_\phi(s)$ are then obtained, after making use of the relations $v' = \cos \theta \sin \psi$ and $w' = -\sin \theta$ (note that, for simplicity in notation, dummy variables of integration are not written explicitly from now on),

$$\omega^2 \int_0^s (F_\theta \sin \psi_e \sin \theta_e - F_\psi \cos \psi_e \cos \theta_e)\, \mathrm{d}s$$

$$= \left\{ \frac{1}{\cos \theta_e \cos \psi_e} (t_1 F_\theta + t_2 F_\phi + t_3 F'_\theta + t_4 F'_\psi + t_5 F'_\phi)' + \frac{\beta_v p_r \left[1 + \dfrac{ml}{M}(1-s) \right]}{\cos \theta_e \cos \psi_e} g_2(s) \right.$$

$$\left. - \omega^2 \tan \psi_e \left[\int_s^1 \int_0^s g_2\, \mathrm{d}s\, \mathrm{d}s + \frac{M}{ml} \int_0^1 g_2\, \mathrm{d}s \right]' \right\} \triangleq F'_{G_{rs}}(s),$$

$$\omega^2 \int_0^s F_\theta \cos \theta_e\, \mathrm{d}s$$

$$= \left\{ -\beta_v p_r \left[1 + \frac{ml}{M}(1-s) \right] \left(F_\theta \frac{\sin \psi_e}{\cos^2 \theta_e} + F_\psi \cos \psi_e \tan \theta_e \right) - F_{G_{rs}}(\sin \psi_e \tan \theta_e) \right.$$

$$- \frac{1}{\cos \theta_e} [(t_6 F_\theta + t_7 F_\phi + t_8 F'_\theta + t_3 F'_\psi)' + t_9 F_\theta + t_{10} F_\phi - t_6 F'_\theta - t_1 F'_\psi + t_{11} F'_\phi]$$

$$\left. + \omega^2 \cos \psi_e \tan \theta_e \left[\int_s^1 \int_0^s g_2\, \mathrm{d}s\, \mathrm{d}s + \frac{M}{ml} \int_0^1 g_2\, \mathrm{d}s \right]' \right\} \triangleq F'_{G_{ws}}(s)$$

$$\beta_\zeta F''_\phi - t_5 F''_\psi + t_{12} F_\theta + t_{13} F_\phi + t_{14} F'_\theta + t_{15} F'_\psi = 0. \tag{27}$$

In eqns (27),

$$g_2(s) = F_\psi \sin \psi_e \cos \theta_e + F_\theta \cos \psi_e \sin \theta_e. \tag{28}$$

The cantilever boundary conditions for eqns (27) are

$$F_\theta(0) = F_\psi(0) = F_\phi(0) = F_\theta'(1) = F_\psi'(1) = F_\phi'(1) = 0,$$

$$F_{G_{rs}}(1) = \omega^2 \frac{M}{ml} \int_0^1 (F_\psi \cos \psi_e \cos \theta_e - F_\theta \sin \psi_e \sin \theta_e)\, ds$$

and

$$F_{G_{ws}}(1) = -\omega^2 \frac{M}{ml} \int_0^1 F_\theta \cos \theta_e\, ds.$$

The eigenfunctions $F_\psi(s)$, $F_\theta(s)$ and $F_\phi(s)$, and the frequencies ω_i, are obtained by direct integration of eqns (27). For this, a set of state variables is introduced so that these integro-differential equations are written as a set of ordinary differential equations. The following states are defined:

$$x_1 = F_\theta; \quad x_2 = F_\psi; \quad x_3 = F_\phi$$

$$x_4 = \int_0^s (F_\theta \sin \psi_e \sin \theta_e - F_\psi \cos \psi_e \cos \theta_e)\, ds$$

$$x_5 = \int_0^s (F_\theta \cos \psi_e \sin \theta_e + F_\psi \sin \psi_e \cos \theta_e)\, ds$$

$$x_6 = \int_0^s F_\theta \cos \theta_e\, ds$$

$$x_7 = F_\theta'; \quad x_8 = F_\psi'; \quad x_9 = F_\phi'$$

$$x_{10} = -\int_s^1 x_5\, ds$$

$$x_{11} = F_{G_{rs}} + \frac{\omega^2 M}{ml} x_4$$

$$x_{12} = F_{G_{ws}} + \frac{\omega^2 M}{ml} x_6. \tag{29}$$

The cantilever boundary conditions for these states are $x_i(0) = 0$ for $i = 1, \ldots, 6$, and $x_j(1) = 0$ for $j = 7, \ldots, 12$.

Defining

$$\mathbf{x} = [x_1, \ldots, x_6; x_7, \ldots, x_{12}]^\mathrm{T} \triangleq \begin{bmatrix} \mathbf{y}_1 \\ \mathbf{y}_2 \end{bmatrix} \tag{30}$$

where $\mathbf{y}_1$ and $\mathbf{y}_2$ are, respectively, 6×1 columns with $\mathbf{y}_1(0) = 0$ and $\mathbf{y}_2(1) = 0$, eqns (27) can be written as

$$\mathbf{x}'(s) = A(s)\mathbf{x}(s) + B(s)\mathbf{x}(1). \tag{31}$$

All the elements $B_{i,j}$ of the 12×12 matrix B are zero, except $B_{7,5}$, $B_{8,5}$ and $B_{9,5}$.

The solution to eqn (31) is

$$\mathbf{x}(s) = \Phi(s)\mathbf{x}(0) + \left[\Phi(s) \int_0^s \Phi^{-1}(\tau)B(\tau)\, d\tau\right]\mathbf{x}(1), \tag{32}$$

where $\Phi(s)$ satisifes the differential equation

$$\Phi'(s) = A(s)\Phi(s) \tag{33}$$

with the initial condition $\Phi(0) = I$, the 12×12 identity matrix. Also, it is easily verified that

$$F(s) \triangleq \Phi(s) \int_0^s \Phi^{-1}(\tau)B(\tau)\,d\tau \tag{34}$$

satisfies the differential equation

$$F'(s) = A(s)F(s) + B(s) \tag{35}$$

with $F(0) = 0$, the 12×12 null matrix. Only the three elements $B_{7,5}$, $B_{8,5}$ and $B_{9,5}$ in column five of the matrix $B(s)$ are non-zero.

From eqn (32) one obtains,

$$x(1) = \begin{bmatrix} y_1(1) \\ 0 \end{bmatrix} = [I - F(1)]^{-1}\Phi(1)\begin{bmatrix} 0 \\ y_2(0) \end{bmatrix} \triangleq \begin{bmatrix} K_{1,1} & K_{1,2} \\ K_{2,1} & K_{2,2} \end{bmatrix}\begin{bmatrix} 0 \\ y_2(0) \end{bmatrix}. \tag{36}$$

Equation (36) discloses that for $y_2(0)$ to be non-zero the characteristic equation $\det K_{2,2} = 0$ for the 6×6 "transfer matrix" $K_{2,2}$ has to be satisfied. The methodology presented above provides an iterative technique for determining the natural frequencies, ω. For this, one chooses a starting value ω^* for ω, integrates eqns (33) and (35) numerically from $s = 0$ to $s = 1$, calculates $\det(K_{2,2})$, which is dependent on ω, and then iterates on the value of ω until $|\det K_{2,2}|$ is smaller than a small pre-assigned quantity. This procedure was implemented using the IMSL package (IMSL, 1987) on a Sun 3 series computer. For chosen values of

$$\left(\beta_y, \beta_z, P, \frac{M}{ml} = \frac{D_n}{mgl^3}, P\right),$$

ω was determined as a function of α by using the double precision IMSL routine DZREAL to find the real zeros ω, of the function defined as $\det(K_{2,2}(\omega))$. The routine DZREAL has two convergence criteria. The first requires that the magnitude of the function be less than a pre-selected value ERRABS, and the second requires that the relative change of two successive approximations for ω be less than another pre-selected value, ERREL. Convergence is achieved when either criterion is satisfied. The results obtained were essentially insensitive to values of ERRABS and ERREL between 10^{-4} and 10^{-10}. To determine $K_{2,2}$, each of the 12 columns $u_i(s)$ of eqn (33) was integrated from $s = 0$ to $s = 1$, with all the elements of $u_i(0)$ equal to zero except the one in the *i*th row. Integration of three more differential equations, given by the fifth column of eqn (35), was performed to determine the fifth column of the matrix $F(1)$. The double precision IMSL routine DIVPAG, which uses an implicit Adams–Moulton algorithm, was used to integrate the differential equations with an error control parameter set to 10^{-10}. Again, no noticeable changes in the results were detected for values of that control parameter as low as 10^{-4}.

A discussion of all the results is presented after the next section, where an alternative calculation of the frequencies is presented and its validity is then assessed.

RESPONSE ANALYSIS BASED ON APPROXIMATE EQUATIONS OF MOTION EXPANDED ABOUT THE UNDEFORMED STATE

Equations (11) are valid for arbitrarily large deformations, as long as the strains are infinitesimally small. An alternative technique to analyze the motion, valid for "small" motions, consists of letting $r(s,t) = \varepsilon r_1(s,t)$ and $w(s,t) = \varepsilon w_1(s,t)$ in eqns (11), with $\phi = O(\varepsilon^2)$ obtained from eqn (14) in terms of $r(s,t)$ and $w(s,t)$, and then expanding eqns

(11) **at least to** $O(\varepsilon^3)$. The resulting equations are then used to analyze the motion of the beam. The $O(\varepsilon^3)$ expanded equations, obtained as indicated above, are given below. The book-keeping parameter ε, and the subscripts are omitted for convenience in the notation:

$$
G_c' = \left\{ -\beta_y v''' - (1-\beta_y)\left[w'' \int_s^1 v'' w'' \, ds + w''' \int_0^s v'' w' \, ds \right] \right.
$$

$$
+ \frac{(1-\beta_y)^2}{\beta_z}\left[w'' \int_0^s \int_s^1 v'' w'' \, ds \, ds \right]' - \beta_z v'(v' v'' + w' w'')'
$$

$$
\left. + \frac{v'}{2} \int_s^1 \left[\int_0^s (v'^2 + w'^2) \, ds \right]^{\cdot\cdot} ds + \frac{M}{2ml} v' \int_0^1 (v'^2 + w'^2)^{\cdot\cdot} \, ds \right\}' = \ddot{v} - \frac{ml}{M} \beta_y p_c
$$

$$
G_w' = \left\{ -w''' + (1-\beta_y)\left[v'' \int_s^1 v'' w'' \, ds + v''' \int_0^s w'' v' \, ds \right] \right.
$$

$$
+ \frac{(1-\beta_y)^2}{\beta_z}\left[v'' \int_0^s \int_s^1 v'' w'' \, ds \, ds \right]' - w'(v' v'' + w' w'')'
$$

$$
\left. + \frac{w'}{2} \int_s^1 \left[\int_0^s (v'^2 + w'^2) \, ds \right]^{\cdot\cdot} ds + \frac{M}{2ml} w' \int_0^1 (v'^2 + w'^2)^{\cdot\cdot} \, ds \right\}' = \ddot{w} - \frac{ml}{M} p_w. \tag{37}
$$

The boundary conditions for these equations are

$$
v(0,t) = w(0,t) = v'(0,t) = w'(0,t) = 0, \quad v''(1,t) = w''(1,t) = 0,
$$

$$
G_w(1,t) = p_w - \frac{M}{ml}\ddot{w}(1,t) \quad \text{and} \quad G_c(1,t) = \beta_y p_c - \frac{M}{ml}\ddot{v}(1,t).
$$

The $O(\varepsilon^1)$ equilibrium solution to the above equations is given by eqns (20). By perturbing the equilibrium solution as

$$
v(s,t) = v_e(s) + v_s(s,t)
$$

$$
w(s,t) = w_e(s) + w_s(s,t), \tag{38}
$$

eqns (37) are linearized in the infinitesimally small perturbations, $v_s(s,t)$ and $w_s(s,t)$. By letting $v(s,t) = F_v(s) e^{i\omega t}$ and $w_s(s,t) = F_w(s) e^{i\omega t}$, the following linear integro-differential equations are obtained for the functions $F_v(s)$ and $F_w(s)$,

$$
-\omega^2 F_v = \left\{ -\beta_y F_v''' - (1-\beta_y)\left[w_e'' \int_s^1 (v_e'' F_w'' + w_e'' F_v'') \, ds \right. \right.
$$

$$
\left. - F_w'' I_1(s) + w_e''' \int_0^s (v_e'' F_w' + w_e' F_v'') \, ds + F_w''' I_2(s) \right]
$$

$$
+ \frac{(1-\beta_y)^2}{\beta_z}\left[w_e'' \int_0^s \int_s^1 (v_e'' F_w'' + w_e'' F_v'') \, ds \, ds - F_w'' I_3(s) \right]'
$$

$$
- \beta_y v_e'(v_e' F_v'' + v_e'' F_v' + w_e' F_w'' + w_e'' F_w')' - \beta_y(v_e' v_e'' + w_e' w_e'')' F_v'
$$

$$
\left. - \omega^2 v_e' \int_s^1 \int_0^s (v_e' F_v' + w_e' F_w') \, ds \, ds - \frac{M}{ml} \omega^2 v_e' \int_0^1 (v_e' F_v' + w_e' F_w') \, ds \right\}' \triangleq G_{vs}'(s),
$$

$$-\omega^2 F_w = \left\{ -F_w''' + (1-\beta_y)\left[v_e'' \int_s^1 (v_e'' F_w'' + w_e'' F_r'') \, ds - F_r'' I_1(s) \right.\right.$$

$$+ v_e''' \left(v_e' F_w + w_e' F_r - \int_0^s (v_e'' F_w + w_e' F_r'') \, ds \right) + F_r''' [v_e' w_e' - I_2(s)] \right]$$

$$+ \frac{(1-\beta_y)^2}{\beta_z}\left[v_e'' \int_0^s \int_s^1 (v_e'' F_w'' + w_e'' F_r'') \, ds \, ds - F_r'' I_3(s) \right]'$$

$$- w_e'(v_e' F_r'' + v_e'' F_r' + w_e' F_w'' + w_e'' F_w')' - (v_e' v_e'' + w_e' w_e'')' F_w$$

$$\left. - \omega^2 w_e' \int_s^1 \int_0^s (v_e' F_r' + w_e' F_w') \, ds \, ds - \frac{M}{ml} \omega^2 w_e' \int_0^1 (v_e' F_r' + w_e' F_w') \, ds \right\}' \triangleq G_{ws}'(s),$$

$$\tag{39}$$

where

$$I_1(s) = -\int_s^1 v_e'' w_e'' \, ds$$

$$I_2(s) = \int_0^s v_e'' w_e' \, ds$$

$$I_3(s) = \int_0^s I_1 \, ds. \tag{40}$$

The cantilever boundary conditions for eqns (39) are

$$F_r(0) = F_w(0) = F_r'(0) = F_w'(0) = 0, \quad F_r''(1) = F_w''(1) = 0,$$

$$G_{rs}(1) = \frac{M}{ml} \omega^2 F_r(1) \quad \text{and} \quad G_{ws}(1) = \frac{M}{ml} \omega^2 F_w(1).$$

As in the previous section, a set of state variables is introduced to reduce eqns (39) to a set of ordinary differential equations that is integrated numerically to determine the frequencies ω_i. The following state variables are defined:

$$x_1 = F_r; \quad x_2 = F_r'; \quad x_3 = F_w; \quad x_4 = F_w'$$

$$x_5 = \int_0^s [v_e' F_r' + w_e' F_w'] \, ds$$

$$x_6 = \int_0^s [v_e'' F_w' + w_e' F_r''] \, ds$$

$$x_7 = \int_0^s \int_1^r [v_e'' F_w'' + w_e'' F_r''] \, ds \, ds; \quad x_8 = F_r''; \quad x_9 = F_w''$$

$$x_{10} = \int_1^s [v_e'' F_w'' + w_e'' F_r''] \, ds; \quad x_{11} = \int_1^s x_5 \, ds$$

$$x_{12} = G_{rs}(s) - \frac{M}{ml} \omega^2 F_r(s); \quad x_{13} = G_{ws}(s) - \frac{M}{ml} \omega^2 F_w(s). \tag{41}$$

Defining

$$\mathbf{x} = [x_1, \ldots, x_7 : x_8, \ldots, x_{13}]^T \triangleq \begin{bmatrix} \mathbf{y}_1 \\ \mathbf{y}_2 \end{bmatrix} \tag{42}$$
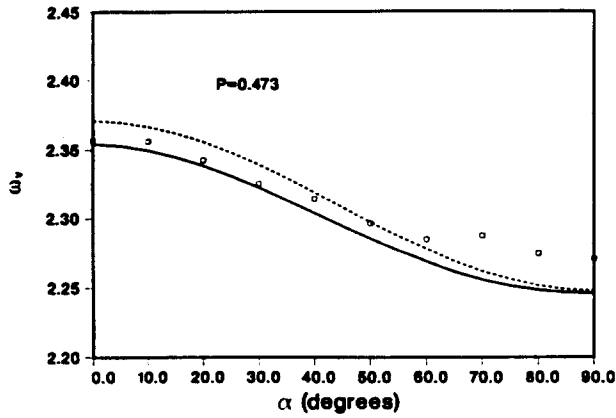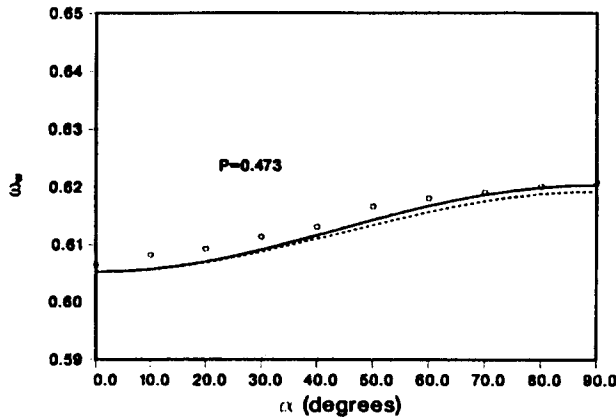
Fig. 6. Natural frequency ω_r for $P = 0.473$ and $D_q/(mgl^1) = 16.69$ [———— eqns (27) with the equilibrium E given by eqns (17) and (18); — — — — — eqn (27) with the $O(\varepsilon^1)$ equilibrium E^* given by eqns (20) and (22); - - - approximate analysis based on eqns (39)].

Fig. 7. Natural frequency ω_s for $P = 0.473$ and $D_q/(mgl^1) = 16.69$ [———— eqns (27) with the equilibrium E given by eqns (17) and (18); — — — — — eqn (27) with the $O(\varepsilon^1)$ equilibrium E^* given by eqns (20) and (22); - - - approximate analysis based on eqns (39)].

where y_1 and y_2 are, respectively, 7×1 and 6×1 columns with $y_1(0) = 0$ and $y_2(1) = 0$, eqns (39) are put in the same form as eqn (31). Here, all the elements $B_{i,j}$ of the 13×13 matrix B are zero, except $B_{8,5}$ and $B_{9,5}$. These elements are readily obtained when the expressions for G_{vs} and G_{ws} given by eqns (39) are written in terms of the state variables defined above. They are given as

$$\begin{bmatrix} B_{8,5} \\ B_{9,5} \end{bmatrix} = -\frac{M\omega^2}{ml} \begin{bmatrix} \beta_y(1+v_e'^2) & (1-\beta_y)I_2 + \dfrac{(1-\beta_y)^2}{\beta_y} I_3 + \beta_y v_e' w_e' \\ (1-\beta_y)(I_2 - v_e' w_e') & 1 + w_e'^2 \\ + \dfrac{(1-\beta_y)^2}{\beta_y} I_3 + v_e' w_e' & \end{bmatrix}^{-1} \begin{bmatrix} v_e' \\ w_e' \end{bmatrix}. \quad (43)$$

From this point on, the natural frequencies ω_i were calculated in the same manner as described at the end of the previous section.

ADDITIONAL RESULTS AND DISCUSSION

Numerical results have been obtained for the natural frequencies associated with the first two coupled flexural modes. We denote by ω_r the natural frequency for the mode
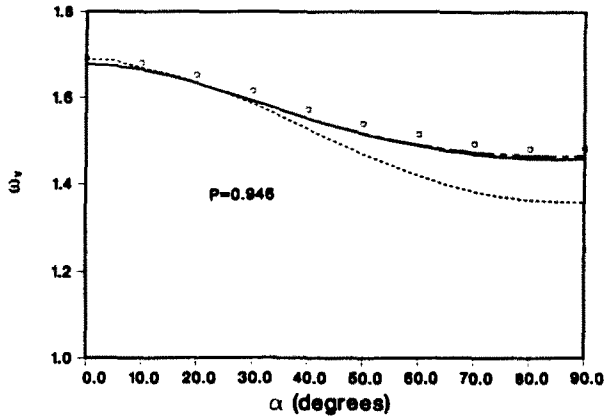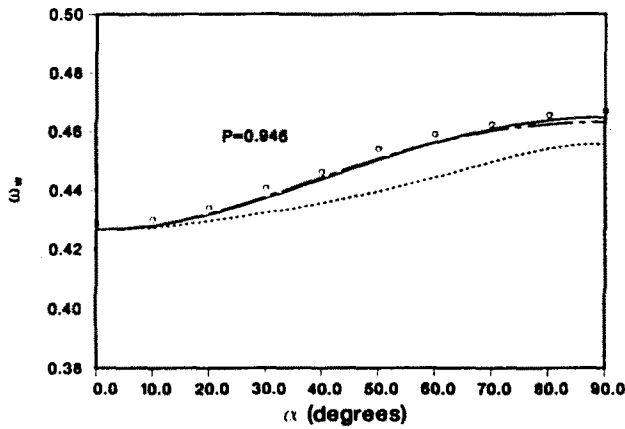
Fig. 8. Natural frequency ω_v for $P = 0.946$ and $D_\eta/(mgl^3) = 16.69$ [——— eqns (27) with the equilibrium E given by eqns (17) and (18) ; — — — — — eqn (27) with the $O(\varepsilon^3)$ equilibrium E^* given by eqns (20) and (22) ; - - - approximate analysis based on eqns (39)].

Fig. 9. Natural frequency ω_u for $P = 0.946$ and $D_\eta/(mgl^3) = 16.69$ [——— eqns (27) with the equilibrium E given by eqns (17) and (18) ; — — — — — eqn (27) with the $O(\varepsilon^3)$ equilibrium E^* given by eqns (20) and (22) ; - - - approximate analysis based on eqns (39)].
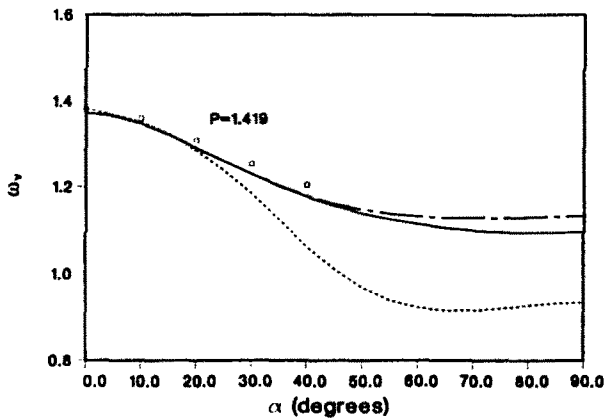

Fig. 10. Natural frequency ω_v for $P = 1.419$ and $D_\eta/(mgl^3) = 16.69$ [——— eqns (27) with the equilibrium E given by eqns (17) and (18) ; — — — — — eqn (27) with the $O(\varepsilon^3)$ equilibrium E^* given by eqns (20) and (22) ; - - - approximate analysis based on eqns (39)].

dominated by the edgewise deflection, and by ω_w the natural frequency dominated by the flatwise deflection. Figures 6–11 show plots of ω_v and ω_w versus α for the same parameter values used to determine the static equilibrium state, and for $D_\eta/(mgl^3) = 16.69$. The value chosen for $D_\eta/(mgl^3)$, matches that for the beam used in the experiments mentioned earlier (the experimental points are indicated by circles in Figs 6–11). The values of ω, in Hertz,
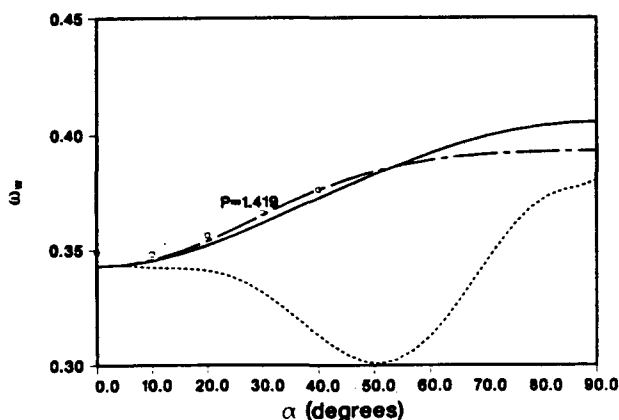
Fig. 11. Natural frequency ω_n for $P = 1.419$ and $D_\eta (mgl^3) = 16.69$ [——— eqns (27) with the equilibrium E given by eqns (17) and (18); — — — — — eqn (27) with the $O(\varepsilon^3)$ equilibrium E^* given by eqns (20) and (22); - - - approximate analysis based on eqns (39)].

for that beam are obtained by multiplying the non-dimensional values of ω by 2.86. These plots show the frequencies obtained as indicated in the previous two sections. The solid lines show the correct natural frequencies obtained from eqns (27) with the equilibrium solution E given by the numerical solution to eqns (17) and (18). However, only slight changes in the natural frequencies determined from such equations occur if one uses, in those equations, the $O(\varepsilon^3)$ approximation, E^*, for the equilibrium solution given by eqns (20) and (22). These approximate results are shown by the — — — lines in Figs 6–11. Even for $P = 1.419$ (i.e. when the weight of the tip mass is about 24 times larger than the weight of the beam) these approximate results are within 3% of the results shown by the solid lines. For the smaller values of P shown in those figures, these approximate results are essentially the same as those represented by the solid lines. All these results are in very close agreement with the experimental points and with the finite element results reported in Hinnant and Hodges (1987) and in Bauchau and Liu (1989). The finite element results are essentially indistinguishable from the results illustrated by the solid lines in the figures under discussion.

The dashed lines - - - shown in Figs 6–11 represent the results obtained by the approximate analysis based on eqns (39), and presented in the previous section. While such approximate results shown in Figs 6–9 exhibit the correct trend, and are within 7% of the correct results for $0 \leqslant \alpha \leqslant \pi/2$, the corresponding results shown in Figs 10 and 11 for $P = 1.419$ are clearly wrong. This is especially evident in the results obtained for the flatwise frequency ω_n shown in Fig. 11 for $P = 1.419$. These results prompted the authors to question the validity of an analysis based on equations expanded about the undeformed state of the beam, when such a state is not an equilibrium (as is the case when P is not zero). For large values of P, replacing the original eqns (11) by the $O(\varepsilon^3)$ eqns (37), expanded about $r = w = \phi = 0$, is not accurate enough to describe the motion about the equilibrium E^*, which represents the same order approximation for the true equilibrium state E.

SUMMARY

The static equilibrium deflections and natural frequencies associated with infinitesimally small oscillations about the static equilibrium, were studied for a cantilevered beam with a heavy tip mass. The following three points summarize the conclusions in this study:

(1) The static equilibrium state due to coupled flexure and torsion of an inextensional beam with a heavy tip mass, was determined by both a numerical two-point boundary value solver, and by approximate $O(\varepsilon^3)$ and $O(\varepsilon^5)$ perturbation solutions. The numerical equilibrium solution, E, exhibits deflections that are

essentially identical with previously published finite element results, and with experimental data. Furthermore, the deflections exhibited by the perturbation solution, E^*, agree well with the numerical solution for smaller tip masses but deteriorate, as expected, as the tip mass is increased. The maximum error reaches about 8% for the largest tip mass considered, which is about 24 times the mass of the beam. The $O(\varepsilon^5)$ solution shows improvement over the $O(\varepsilon^3)$ solution, resulting in a maximum error of less than 4%.

(2) The frequencies associated with small oscillations about the equilibrium state of the beam have been determined by linearization of the equations of motion about the static equilibrium state, and by using a transfer matrix technique on the resulting equations. The natural frequencies thus obtained were also essentially identical to published finite elements and with experimental results. The effect on the calculated frequencies of using the approximate solution E^*, obtained by a perturbation method (instead of the more exact numerical solution E mentioned above) in the linearized equations, was also determined. The use of E^* instead of E results in frequencies that differ only slightly from the "exact" ones with the error becoming larger as the tip mass is increased. However, even for the largest tip mass considered, the differences are less than 3%.

(3) The use of an alternative way to determine an approximation for the natural frequencies of the system was also assessed. For this, small deflections from the undeformed state were assumed, and the equations of motion were expanded about the undeformed state (which is not an equilibrium solution) of the beam. The resulting equations, which contain only polynomial nonlinearities, were then used to analyze the motion. An approximate equilibrium solution to these equations was determined by a perturbation expansion and is identical to E^*. However, when these equations are linearized about E^*, the natural frequencies (again determined by a transfer matrix technique) can be in error by a considerable amount, especially for large values of the tip mass. It is concluded that this type of approximation, which is quite common in the engineering literature, is not suitable, in general, unless one keeps terms of a much higher order in the expanded equations. It is emphasized that the error introduced in this approximate analysis is due essentially to approximating the full nonlinear differential equations prior to the linearization process, rather than the use of an approximate equilibrium solution.

REFERENCES

Bauchau, O. A. and Liu, S. P. (1989). Finite element based modal analysis of helicopter rotor blades. *Vertica* 13, 197-206.
Crespo da Silva, M. R. M. (1988a). Nonlinear flexural-flexural-torsional-extensional dynamics of beams. I: Formulation. *Int. J. Solids Structures* 24, 1225-1234.
Crespo da Silva, M. R. M. (1988b). Nonlinear flexural-flexural-torsional-extensional dynamics of beams. II: Response analysis. *Int. J. Solids Structures* 24, 1235-1242.
Crespo da Silva, M. R. M. and Glynn, C. C. (1978a). Nonlinear flexural-flexural-torsional dynamics of inextensional beams. I: Equations of motion. *J. Struct. Mech.* 6, 437-448.
Crespo da Silva, M. R. M. and Glynn, C. C. (1987b). Nonlinear flexural-flexural-torsional dynamics of inextensional beams. II: Forced motions. *J. Struct. Mech.* 6, 449-461.
Crespo da Silva, M. R. M. and Hodges, D. H. (1986). Nonlinear flexure and torsion of rotating beams, with application to helicopter rotor blades. II: Response and stability analysis. *Vertica* 2, 171-186.
Dowell, E. H. and Traybar, J. (1975a). An experimental study of the nonlinear stiffness of a rotor blade undergoing flap, lag and twisting deformations. AMS Report No. 1194, Department of Aerospace and Mechanical Sciences, Princeton University, NJ.
Dowell, E. H. and Traybar, J. (1975b). An experimental study of the nonlinear stiffness of a rotor blade undergoing flap, lag and twisting deformations. AMS Report No. 1257, Department of Aerospace and Mechanical Sciences, Princeton University, NJ.

Dowell. E. H.. Traybar. J. and Hodges. D. H. (1977). An experimental–theoretical correlation study of nonlinear bending and torsion deformations of a cantilever beam. *J. Sound Vibr.* **50**, 533–544.

Hinnant. H. E. and Hodges. D. H. (1987). Nonlinear analysis of a cantilever beam. *AIAA Jl* **26**, 1521–1527.

Hodges. D. H.. Crespo da Silva. M. R. M. and Peters D. A. (1988). Nonlinear effects in the static and dynamic behavior of beams and rotor blades. *Vertica* **12**, 243–256.

Hodges. D. H. and Ormiston. R. A. (1976). Stability of elastic bending and torsion of uniform cantilever rotor blades in hover with variable structural coupling. NASA TN D-8192.

IMSL (1987). *Math Library User's Manual.* IMSL. Houston. Texas.

Ormiston. R. A. and Hodges. D. H. (1972). Linear flap-lag dynamics of helicopter rotor blades in hover. *J. Amer. Hel. Soc.* **17**(2), 2–14.

Pavelle. R. and Wang. P. S. (1985). MACSYMA from F to G. *J. Sym. Compn* **1**, 69–100.

Rand. R. H. (1984). *Computer Algebra in Applied Mathematics: An Introduction to MACSYMA.* Pitman. Boston. MA.

Symbolics (1987). *MACSYMA User's Guide.* Symbolics. Burlington. MA.

APPENDIX: COEFFICIENTS t_i FOR EQNS (24) AND (27)

$$t_1 = (1 - \beta_x)\theta_c'(\sin 2\phi_c \sin \theta_c)/2 + \beta_x \phi_c' \cos \theta_c + (\sin^2 \phi_c + \beta_x \cos^2 \phi_c - \beta_z)\psi_c' \sin 2\theta_c$$

$$t_2 = (\beta_x - 1)(\psi_c' \sin 2\phi_c \cos \theta_c + \theta_c' \cos 2\phi_c) \cos \theta_c$$

$$t_3 = (\beta_x - 1)(\sin 2\phi_c \cos \theta_c)/2$$

$$t_4 = -\beta_x \sin^2 \theta_c - (\sin^2 \phi_c + \beta_x \cos^2 \phi_c) \cos^2 \theta_c$$

$$t_5 = \beta_x \sin \theta_c$$

$$t_6 = (1 - \beta_x)\psi_c'(\sin 2\phi_c \sin \theta_c)/2$$

$$t_7 = (1 - \beta_x)(\theta_c' \sin 2\phi_c - \psi_c' \cos 2\phi_c \cos \theta_c)$$

$$t_8 = -\beta_x \sin^2 \phi_c - \cos^2 \phi_c$$

$$t_9 = (\beta_x - 1)\psi_c'\theta_c'(\sin 2\phi_c \cos \theta_c)/2 + \beta_x \psi_c'\phi_c' \sin \theta_c - (\beta_x \cos^2 \phi_c + \sin^2 \phi_c - \beta_z)\psi_c'^2 \cos 2\theta_c + A_0 \tan \theta_c$$

$$t_{10} = (\beta_x - 1)(\psi_c' \sin 2\phi_c \cos \theta_c + \theta_c' \cos 2\phi_c)\psi_c' \sin \theta_c$$

$$t_{11} = -\beta_x \psi_c' \cos \theta_c$$

$$t_{12} = -t_{10} - \beta_x(\psi_c' \cos \theta_c)'$$

$$t_{13} = (\beta_x - 1)[(\psi_c'^2 \cos^2 \theta_c - \theta_c'^2) \cos 2\phi_c - 2\psi_c'\theta_c' \sin 2\phi_c \cos \theta_c]$$

$$t_{14} = t_7 - \beta_x \psi_c' \cos \theta_c$$

$$t_{15} = [(\beta_x - 1)(\psi_c' \sin 2\phi_c \cos \theta_c + \theta_c' \cos 2\phi_c) - \beta_x \theta_c'] \cos \theta_c \qquad \text{(A1–A15)}$$